Published in final edited form as:

Cell Rep. 2024 August 27; 43(8): 114611. doi:10.1016/j.celrep.2024.114611.

Vocalization modulates the mouse auditory cortex even in the absence of hearing

Thomas C. Harmon[1,5,*], **Seth Madlon-Kay**[1,2], **John Pearson**[1,2,3], **Richard Mooney**[1,4]

[1]Department of Neurobiology, Duke University, Durham, NC 27710, USA

[2]Center for Cognitive Neuroscience, Duke University, Durham, NC 27708, USA

[3]Department of Biostatistics & Bioinformatics, Duke University, Durham, NC 27710, USA

[4]Senior author

[5]Lead contact

SUMMARY

Vocal communication depends on distinguishing self-generated vocalizations from other sounds. Vocal motor corollary discharge (CD) signals are thought to support this ability by adaptively suppressing auditory cortical responses to auditory feedback. One challenge is that vocalizations, especially those produced during courtship and other social interactions, are accompanied by other movements and are emitted during a state of heightened arousal, factors that could potentially modulate auditory cortical activity. Here, we monitor auditory cortical activity, ultrasonic vocalizations (USVs), and other non-vocal courtship behaviors in a head-fixed male mouse while he interacts with a female mouse. This approach reveals a vocalization-specific signature in the auditory cortex that suppresses the activity of USV playback-excited neurons, emerges before vocal onset, and scales with USV band power. Notably, this vocal modulatory signature is also present in the auditory cortex of congenitally deaf mice, revealing an adaptive vocal CD signal that manifests independently of auditory feedback or auditory experience.

In brief

Harmon et al. find that vocalization suppresses the auditory cortex, a modulatory effect distinct from modulation by locomotion or female odorants. Moreover, vocal modulation scales with vocal acoustic properties in both hearing and deaf mice, pointing to corollary discharge signals that anticipate vocal properties even in the absence of hearing.

*Correspondence: thomas.harmon@duke.edu.

AUTHOR CONTRIBUTIONS

Conceptualization, T.C.H. and R.M.; methodology, T.C.H.; software, T.C.H. and S.M.-K.; validation, T.C.H. and S.M.-K.; formal analysis, T.C.H. and S.M.-K.; investigation, T.C.H.; resources, J.P. and R.M.; data curation, T.C.H.; writing – original draft, T.C.H. and R.M.; writing – review & editing, T.C.H., S.M.-K., J.P., and R.M.; visualization, T.C.H.; supervision, J.P. and R.M.; project administration, J.P. and R.M.; funding acquisition, T.C.H. and R.M.

DECLARATION OF INTERESTS

The authors declare no competing interests.

SUPPLEMENTAL INFORMATION

Supplemental information can be found online at https://doi.org/10.1016/j.celrep.2024.114611.

Graphical abstract

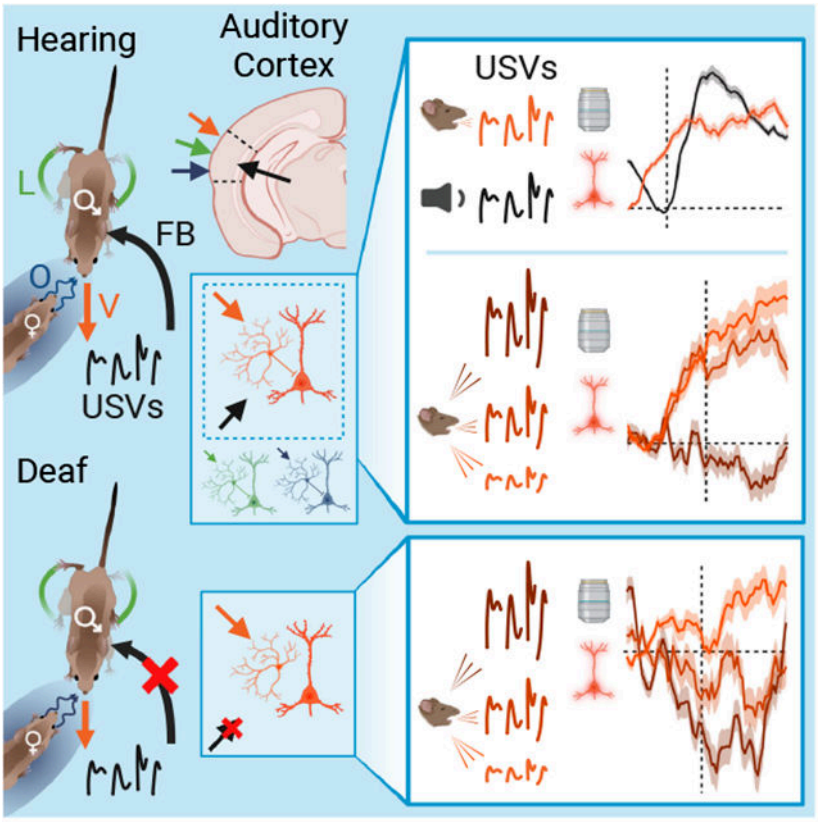

INTRODUCTION

Vocalization is an essential medium for communication in all mammals. To facilitate hearing during vocal production, the auditory system must distinguish the organism's own vocalization-related auditory feedback (vocal feedback) from other sounds. Corollary discharge (CD) signals that adaptively suppress auditory cortical responses to vocal feedback are theorized to facilitate this distinction. This theory is supported by the observation that auditory cortical activity in vocalizing monkeys and humans is suppressed relative to auditory cortical responses evoked by vocal playback.[1–13] While this suppressive signature is consistent with modulation by a vocal-motor CD signal, a potential confound is that vocalizations, especially those produced during courtship and other social interactions, are not produced as an isolated behavior. Instead, vocalizations in these contexts are elicited by social cues, reflect a heightened state of arousal, and are emitted in concert with other movements, any or all of which could potentially modulate auditory cortical activity.[14–18] Therefore, determining whether vocalization-specific signals modulate auditory cortical activity requires systematically monitoring these additional factors while measuring auditory cortical activity during vocalization.

The mouse provides the potential for disentangling this problem: male mice produce courtship ultrasonic vocalizations (USVs) in response to female odorants and during

a state characterized by high levels of locomotor activity, orofacial movements, and arousal, all of which can also exert modulatory effects on auditory cortical activity.[14–29] Furthermore, numerous studies in mice show a strong modulatory influence of locomotion and other movements on auditory cortical activity, mediated in part by motor-related CD signals.[14,18,30–37] This modulation manifests as a broad suppression of responses to acoustic stimuli during a variety of movements, including locomotion and vocalization.[14] These suppressive signals can be conditioned to adaptively filter out predictable acoustic features of movement-related feedback, indicating that they can be influenced by auditory experience.[30,33,38] Nonetheless, whether an adaptive vocalization-specific CD signal operates in the mouse auditory cortex and the extent to which it depends on vocal feedback experience are unknown.

To resolve these issues, we monitored auditory cortical activity, USV production, and other non-vocal courtship behaviors in a head-fixed male mouse while we controlled its access to a female mouse or female odors. Employing this approach in hearing male mice revealed a vocalization-specific modulatory signature in the auditory cortex that was tightly linked to USV onset and distinct from the modulatory effects of locomotion, female odor, or acute changes in arousal. Vocal modulation often preceded USV onset and, in hearing mice, strongly suppressed the activity of auditory cortical neurons, including many that were otherwise excited by USV playback during non-vocal epochs. Remarkably, similar vocalization-specific modulatory signals were also present in the auditory cortex of congenitally deaf mice. In both hearing and deaf mice, the magnitude of vocal modulation scaled with USV band power, revealing an adaptive vocal CD signal in the mouse auditory cortex that develops independent of auditory experience.

RESULTS

Vocalization suppresses auditory cortical neurons that respond to USV playback

To characterize how vocalization modulates auditory cortical activity, we used two-photon methods to image calcium signals from auditory cortical neurons in a head-fixed male mouse as it vocalized or listened to the same or other USVs played through a speaker during non-vocal epochs. The male's vocalizations were elicited by introducing a female mouse into a chamber that allowed the female to approach and investigate the male's snout (Figure 1A). Females that were habituated to this chamber spontaneously entered the approach corridor several times a session (0.49 ± 0.04 approaches/min), resulting in discrete interactions that often elicited USV bouts from the male (31.9% of interactions). We used adeno-associated viral vectors to express GCaMP8s pan-neuronally and used intersectional methods to distinguish *Vgat*$^{+}$ neurons from other neurons (Figure 1B). This approach revealed a cohort of putative *Vgat*$^{-}$ excitatory pyramidal neurons and *Vgat*$^{+}$ inhibitory interneurons that were excited by USV playback. These same neurons were less excited during vocalization (Figure 1C), a dichotomy that persisted even when we used the male's own vocalizations as playback stimuli (Figure S1). Thus, auditory cortical responses to vocal feedback are suppressed in the mouse, consistent with a vocal CD mechanism.

Vocalization modulates many auditory cortical neurons

One limitation of this initial analysis is that it characterized vocalization-related activity in the relatively small subset of auditory cortical pyramidal neurons (23.5%) and interneurons (22.7%) that responded to USV playback. To determine whether vocalization modulates auditory cortical activity more broadly, we measured the difference in fluorescence during vocal and non-vocal interactions with the female and compared the difference to a null distribution constructed by permuting "vocal" and "non-vocal" labels of behavioral epochs (Figure 1D). When averaged across all vocal epochs, the fluorescence of most auditory cortical pyramidal neurons (58.2%) and interneurons (64.2%) either decreased or increased (Figure 1E). Compared to neurons for which the fluorescence increased (20%) or did not change (22%) during vocalization, auditory cortical neurons with decreased fluorescence were more likely to be excited by USV playback (28.6%, Figures S2A–S2C). Furthermore, neurons that increased their fluorescence during vocalization were excited by a greater proportion of USV playback stimuli than were other auditory cortical neurons (Figure S2D). Therefore, vocalization modulates most auditory cortical neurons, including many that are excited by USV playback.

In many neurons, vocal modulation preceded vocal onset, indicating that it is not simply a consequence of auditory feedback. On average, interneurons that were activated by vocalization responded earlier in the prevocal window than pyramidal neurons (Figure 1E, bottom) but showed less activation following vocal onset. Some neurons showed instances of either activation or suppression just prior to or after vocal onset and no response during other bouts. Other neurons showed more complex vocal modulation, which could involve activation near the onset of vocal bouts and suppression during other bouts (Figure 1F). Thus, vocal modulation of individual auditory cortical neurons is not uniform in timing or sign but instead varies across vocal bouts. By counting episodes of activation and suppression near the onset of vocal bouts, we found that suppression was the dominant mode (Figure 1G), even among neurons whose mean fluorescence was higher during vocal epochs. Beyond the initial 2 s of a vocal bout, vocalization-modulated neurons were often inactive or suppressed. This suppressive or inactive background was punctuated by episodes of activation, resulting in a higher mean fluorescence across all vocal epochs (Figure 1H). In summary, vocal modulation is a common phenomenon in the mouse auditory cortex, comprising increased and/or decreased activity that can emerge prior to vocal onset.

Characterizing social and behavioral variables that accompany vocalization

While these observations raise the possibility that a combination of vocal premotor and feedback signals modulate auditory cortical activity, male mice produce their courtship vocalizations in a dynamic context that includes both vocal and non-vocal behaviors. More specifically, male mice produce courtship USVs while they are aroused and actively pursuing and sniffing the female (Figure 2A). Therefore, a major challenge is distinguishing which of these various factors—vocalization, locomotion, orofacial movements, female odorants, and arousal—modulate auditory cortical activity and whether any of this modulation is vocalization-specific.

To overcome this challenge, we first characterized how social interactions result in male vocalizations by tracking the male-female distance and controlling the male's exposure to female odorants. We accomplished this by regulating the direction that air flowed through the chamber, moving the female to a distal chamber to prevent direct interaction, or simply removing the female altogether. During neutral air flow conditions, males only vocalized when a female was in the proximal chamber. Since the mice were in the dark and could not make direct physical contact, the male's vocalizations are most likely produced in response to female odor. Consistent with this hypothesis, males vocalized most when the female was in the proximal chamber and air flowed toward the male and never vocalized when air flowed away from the male, regardless of the female's proximity (Figure 2B). Lastly, males occasionally vocalized in response to a female located in the distal chamber when airflow was toward the male (Figure 2B, bottom). Therefore, similar to natural courtship, female odorants are a major driver of USV production in head-fixed male mice and are thus a potential modulator of auditory cortical activity during vocalization.

We then exploited our head-fixed preparation to simultaneously record the male's USVs, locomotor activity, orofacial movements, and pupil diameter (a marker of arousal) when the female was either present or absent. This approach revealed that the vocalizing male was invariably running and moving its jaw, whiskers, and snout and that its pupil was dilated to nearly its maximum size during social interactions. Aligning these parameters to vocal onset revealed an acute and subtle locomotor deceleration, increased movements of the jaw but no other facial regions, and no change in pupil diameter (Figure 2C). Thus, the male's USVs are one component of a complex behavioral response to the female that includes locomotion, increased jaw movements, and a heightened state of arousal. While these non-vocal behaviors were evident during interactions with the female that did not elicit vocalizations, their magnitudes were much larger during vocal episodes (Figure 2D). Therefore, in addition to female odorants, locomotor activity, jaw movements, and arousal are potential sources of auditory cortical modulation during vocalization.

Isolating vocalization-specific modulation in the auditory cortex

The preceding behavioral analysis indicates that the male's vocalizations are triggered by female odorants and always accompanied by locomotion. Prior studies have established that both locomotion and odorants can modulate the activity of auditory cortical neurons in the mouse, raising the possibility that the vocal modulation of auditory cortical activity we detected was driven by these other factors and not attributable specifically to vocalization. Therefore, we sought to measure the extent to which locomotor movements and female odorants modulate auditory cortical activity in the male mouse.

We first identified non-vocal epochs during which each of these other sources of modulation was present or absent (Figure 3A). To measure locomotor modulation in the absence of odor modulation, we compared calcium signals of auditory cortical neurons during epochs when the socially isolated male mouse was either running or still. To isolate modulation by female odor from modulation by locomotion, we compared calcium signals from epochs when the male was still and either exposed to air from a distally located female or socially isolated. To identify neurons that were significantly modulated by either of these factors, we compared

the differences in mean fluorescence to null distributions constructed by permuting across epochs during which each modulatory factor was “present” or “absent” (e.g., Figure 1D). This analysis revealed that many auditory cortical neurons are significantly modulated by either locomotion or female odor (Figure 3B). Aligning the calcium signal of locomotion-modulated neurons to locomotion onset revealed modulation in the premotor window, consistent with a locomotion-related CD signal (Figure 3C). While the fluorescence of some vocalization-modulated neurons changed at locomotion onset, the change in fluorescence of these neurons at vocal onset was often larger and of a different sign (Figure 3D). The modulatory effect of odor could not be accounted for by a higher state of arousal in the male, as odor presentation did not reliably produce an increase in pupil size. Furthermore, odor-evoked changes in fluorescence were similar regardless of whether the male was still or running (Figure S3). Therefore, even in the absence of vocalization, both locomotion and female odorants modulate auditory cortical activity in the male mouse, presenting a challenge to determining whether vocal modulation of the auditory cortex is specific to vocalization and not these other factors.

If vocal modulation in the auditory cortex is simply a consequence of locomotion or odorants, then neurons modulated by vocalization should also be subject to strong locomotion or odor modulation of the same sign. Indeed, while a substantial proportion (20.5%) of neurons were modulated only by vocalization, others were modulated by locomotion or odor as well (Figure 3E). However, most combinations that included vocal and non-vocal modulation occurred at or below chance level (Table S1). An exception to this was combinations where vocalization and odor exerted oppositely signed modulatory effects. For instance, a substantial number of neurons (12.3% of all neurons) that were activated by vocalization were also suppressed by odor (Figure 3E, yellow box). The combined modulation of this group of neurons by vocalization and female odorants may help the male mouse detect vocalizations by the female during courtship. Consistent with this possibility, a disproportionate number of these co-modulated neurons responded to USV play back stimuli presented in social isolation (Figures S2E and S2F).

Furthermore, if vocal modulation in the auditory cortex is actually driven by concomitant locomotor activity or exposure to female odorants, then the magnitude of vocal modulation would be expected to positively correlate with the magnitude of locomotion or odor modulation measured during non-vocal epochs. Instead, we found only weak correlations between vocal and locomotor modulation and moderate, negative correlations between vocal and odor modulation (Figures 3E and 3F). Together, these data demonstrate that changes in the activity of auditory cortical neurons during vocalization cannot be attributed to non-vocal factors that accompany vocalization and are instead specifically linked to vocalization.

Vocalization also modulates the auditory cortex in the absence of hearing

Previously, we observed that vocal modulation could arise prior to vocal onset and often resulted in suppression of auditory cortical activity (Figure 1E), features that are consistent with a vocal motor-related CD signal. One expectation of such a vocal CD signal is that it should persist in the absence of vocalization-related auditory feedback. To test this possibility, we imaged calcium activity from the auditory cortex of deaf,

vocalizing transgenic mice (*Tmc1*$^{\Delta/\Delta}$)[39]; these mice lack a functional TMC1 protein, which is essential to mechanoelectrical transduction in cochlear hair cells. We confirmed that adult male *Tmc1*$^{\Delta/\Delta}$ mice are devoid of an auditory brainstem response, indicating complete sensorineural deafness (Figure 4A). We also established that, in the head-fixed preparation, these deaf males showed the same behavioral response to the approach of a female mouse and vocalized readily in the presence of a female mouse or odorants. Finally, applying a variational autoencoder to a large corpus of USVs revealed that the vocal repertoires of age-matched, sibling deaf (*Tmc1*$^{\Delta/\Delta}$) and hearing (*Tmc1*$^{+/\Delta}$) adult male mice were highly similar (Figure 4B).

Similar to hearing mice, permutation tests applied to calcium signals revealed that many auditory cortical neurons in deaf mice are modulated by vocalization, locomotion, or female odor (Figure 4C). As observed in hearing mice, vocal modulation involved strong activation or suppression that frequently began prior to vocal onset (Figures 4D and 4E). Notably, the magnitude of vocal modulation in deaf mice was larger than in hearing mice (Figure 4E). Therefore, a vocalization-specific signal modulates the auditory cortex of deaf mice, consistent with a vocal CD signal.

One difference was that vocalization-modulated neurons were less common in the auditory cortex of deaf mice (Figure 4C). Furthermore, more vocalization-modulated neurons in deaf mice were suppressed rather than activated by vocalization. Indeed, even though the majority of these vocalization modulated neurons could exhibit activation or suppression across vocal bouts, suppression was more common when compared to hearing mice (Figures 4F and 4G). One possible explanation is that vocal feedback in hearing mice provides excitation to the auditory cortex that is counterbalanced by suppressive vocal CD signals. Consequently, in the deaf mouse, vocal suppression dominates auditory cortical activity in the absence of vocal feedback.

While neurons modulated by locomotion or odor were also less common in the auditory cortex of deaf mice, locomotion-modulated neurons were either strongly activated or suppressed at locomotion onset, as observed in hearing mice. In fact, when compared to neurons from hearing mice, locomotion modulation was enhanced in magnitude and occurred at reduced latencies at locomotion onset (Figures 4H and 4I). In contrast to neurons from hearing mice, locomotor modulation positively correlated with vocal modulation across all auditory cortical neurons from deaf mice (Figures 4J and 4K). However, when compared to the population of auditory cortical neurons that were significantly modulated by vocalization only (14.7% of the total population), a much smaller population (4.7%) displayed significant vocal and locomotor modulation of the same sign (Table S1). Furthermore, vocalization-modulated auditory cortical neurons showed no change in fluorescence at locomotion onset (Figure S4). In summary, vocalization modulates auditory cortical activity in the absence of hearing.

Vocal modulation in the mouse auditory cortex adapts to certain acoustic features

A remaining issue is whether vocal modulation of the auditory cortex in the mouse functions adaptively, for instance, by scaling with the frequency or amplitude of the emitted vocalization. Such scaling could explain variability in the sign and timing of vocal

modulation that was revealed by our analysis of single vocal bouts (Figures 1E–1G and 4D–4F). Scaled vocal modulation could arise from the effects of vocal feedback, vocal CD signals, or a combination of these two factors. In hearing mice, we found that neurons that are modulated by vocalization are more likely to be excited by USV playback stimuli (Figure S2C). However, auditory tuning properties can only be measured in hearing mice, which complicates any distinction between vocal feedback and CD signals. Here, we tested whether vocal modulation scaled with power of emitted vocalizations in the USV frequency band (36–96 kHz) in both hearing and deaf mice.

To this end, we categorized the first 2 s of each vocal bout by the USV band power and compared calcium signals during bouts with “low,” “mid,” and “high” band power (Figure 5A). Bouts with high band power typically comprised syllables that were louder or lower in frequency or had complex harmonic structure, the latter of which could be quantified by a higher entropy score (Figure 5B). In hearing mice, vocal modulation in the majority of auditory cortical neurons scaled with the USV band power (Figure 5C). This scaling effect emerged prior to vocal onset and was sustained for the first 2 s of the vocal bout. The magnitude of calcium signals of some (40%) neurons scaled in a manner that was directly correlated with band power, with little to no activity during low-band-power bouts, weak activation during mid bouts, and strong activation during high bouts. The calcium signals of other (19%) neurons were inversely correlated with the band power, with activation during low bouts that transitioned into suppression with increasing band power. Thus, in hearing mice, vocal modulation was most pronounced in auditory cortical neurons that responded to ultrasonic acoustic stimuli, and this modulation scaled with USV band power both before and after vocal onset. These features are consistent with either vocal feedback or an adaptive vocal CD signal.

The same analysis in deaf mice revealed that vocal modulation in the auditory cortex also scaled with band power (Figures 5D and 5E). Most neurons showed no modulation during low band power vocal bouts, moderate modulation during mid bouts, and stronger modulation during high bouts. When compared to neurons from hearing mice, many more auditory cortical neurons in deaf mice showed deepening suppression with increasing band power. These data are consistent with a suppressive vocal CD signal that scales with the amplitude and harmonic complexity of the vocalization.

The prevocal signatures and similar scaling of vocal modulation with USV band power in hearing and deaf mice raises the possibility that vocal CD signals are the major source of vocal modulation in hearing mice. Alternatively, both vocal CD signals and vocalization-related auditory feedback could contribute to vocal modulation in the auditory cortex of hearing mice. In fact, auditory cortical neurons of hearing mice showed significantly weaker trial-based correlations compared to deaf mice, which could arise through bout-to-bout variations in the match between vocal CD signals and vocal feedback (Figure 5F). A further expectation is that the influence of feedback should only be apparent after vocal onset. Indeed, when vocal bouts without activation or suppression were excluded, the magnitude of vocal modulation of auditory cortical pyramidal neurons in hearing mice deviated from that in deaf mice only after vocal onset (Figure 5G). Thus, while neurons in the auditory cortex

of hearing mice are strongly influenced by vocal CD signals, auditory cortical pyramidal neurons also appear to be activated by vocal feedback.

DISCUSSION

Overview

Here, we monitored auditory cortical activity in head-fixed male mice as they vocalized to nearby females and listened to playback of vocalizations and other sounds. By systematically measuring and dissociating contributions of vocal production, locomotion, and female odor, we were able to isolate a vocalization-specific modulatory signal in the male's auditory cortex. While this modulation could involve activation or suppression, a notable feature was that vocalization suppressed activity in neurons that responded to vocal playback when the male was socially isolated. Furthermore, many neurons that were modulated by vocalization also responded to USV playback, and the magnitude of vocal modulation scaled with power in the USV frequency band. Notably, vocal modulation was actually enhanced in the auditory cortex of congenitally deaf mice, where it also scaled with vocal power. The prevocal onset of this modulatory signal, along with its suppressive signature, is strongly reminiscent of vocal CD signals detected in the auditory cortex of humans and non-human primates.

Isolation of vocal and other sources of auditory cortical modulation

By employing a head-fixed approach, we determined that courtship vocalizations of male mice are produced as part of a complex behavioral response that includes locomotion, orofacial movements, and heightened arousal. Furthermore, this approach allowed us to carefully regulate airflow, confirming prior studies showing that female odorants are key drivers of USV production.[24–29] Therefore, one advance of the current study is the systematic measurement of the vocal and non-vocal aspects of the male's courtship behavior, which is currently impractical in unrestrained, freely courting mice. By combining these measurements with statistical inference through permutation tests, we were able to confirm and extend earlier studies that showed that the auditory cortex is remarkably multimodal, as its activity can be modulated by locomotion, arousal, and conspecific odorants.[14–19,21,30,36,37] Notably, this approach allowed us to identify neurons that were modulated by vocalization in the male's auditory cortex. Most of these neurons were not affected by locomotion, though a subset showed modulation by vocalization and locomotion of the same or different sign. Thus, our approach demonstrated distinct modulation by vocalization and locomotion while also revealing interactions between these factors in some auditory cortical neurons.

Because female odorants both triggered USV production and modulated auditory cortical neurons in the male, a possibility is that the vocal modulation we detected was a simple consequence of female odor. However, most vocalization-modulated neurons were insensitive to female odor, and the subset of neurons that were modulated by both factors showed opposing effects, contradicting this idea. While modulation by odor of adult conspecifics has not been described previously, odors of mouse pups have been demonstrated to induce greater sensitivity of auditory cortical neurons to pup calls in

post-partum dams.[21–23] An intriguing possibility is that female odors also increase auditory cortical sensitivity in the male mouse, perhaps to heighten the male's ability to detect vocalizations and other sounds made by the female during courtship.

Potential sources of vocal modulation

Potential sources of vocal modulation in the auditory cortex of the hearing mouse include vocal motor CD, vocalization-related auditory feedback, and vocal proprioceptive signals. Several features point to an influence of vocal motor CD signals in the auditory cortex of the vocalizing male. First, the activity of most vocalization-modulated neurons deviated from baseline hundreds of milliseconds prior to vocal onset (Figures 1E, 4D, and 4F), which is similar to locomotor CD signals in the mouse auditory cortex described here and in prior studies.[14,30,36] Second, vocalization suppressed the activity of many auditory cortical neurons, including those that were excited by USV playback in non-vocalizing epochs. Third, these patterns of vocal modulation, and particularly vocal suppression, were present in congenitally deaf mice.

While these findings point strongly to a vocal motor CD signal, more subtle features hint at the additional influence of auditory feedback. For example, the magnitude of vocal modulation in hearing and deaf mice was similar in the prevocal window and then diverged after vocal onset (Figure 5H), consistent with auditory feedback providing an additional source of vocal modulation to the auditory cortex in hearing mice. Moreover, when compared to responses of unmodulated neurons during non-vocal epochs, vocalization-suppressed neurons in hearing mice were more likely to respond to USV playback, while vocalization-activated neurons more often responded to multiple playback stimuli (Figure S2). Consequently, many vocalization-modulated auditory cortical neurons are equipped to integrate USV-related auditory feedback. In fact, during extended vocal bouts in hearing mice, most vocalization-modulated neurons featured sporadic episodes of activation on a background of inactivity or suppression, consistent with occasional mismatches between suppressive vocal CD signals and excitatory vocal feedback. Lastly, compared to deaf mice, vocal suppression in the auditory cortex of hearing mice was less common and smaller in magnitude, which could be explained by excitatory auditory feedback partly counteracting suppressive, non-auditory vocal signals.

A remaining issue is the nature of these non-auditory signals, which could be either motor related or proprioceptive. While distinguishing between these two types of signals is beyond the scope of this study, prior studies have mapped a projection from the secondary motor cortex (M2) that conveys motor-related CD signals to the auditory cortex.[18] Although these prior studies have focused on the role of these M2-related CD signals in the context of locomotor and forelimb movements, the rodent M2 also contains orofacial and laryngeal representations,[40] both of which are active during vocal production.[41–43] Indeed, we observed that the jaw frequently began to move hundreds of milliseconds prior to the onset of vocalization (Figure 2D), and prior studies have established that the digastric muscle contracts to move the jaw in concert with vocalization in Alston's singing mice.[43] Collectively, these observations support the idea that during vocalization, the M2 transmits vocal motor CD signals that suppress auditory cortical activity.

Innate and adaptive features of vocal modulation in the mouse auditory cortex

In primates, vocal CD signals function adaptively to suppress features of vocal feedback that can be reliably anticipated. In humans, this process is thought to facilitate error detection important to speech learning and maintenance.[5,9–11,13,44,45] Here, we noted that the strength of vocal modulation scaled with vocal power and that this effect was evident prior to vocal onset, consistent with an adaptive, anticipatory process. Remarkably, this scaling effect was also present in the auditory cortex of deaf mice, showing that this adaptive signature does not depend on vocalization-related auditory feedback or even any auditory experience. Such a hardwired mechanism could reflect an efficient solution for suppressing feedback of innate vocalizations, which, as shown here and in prior studies, develop uniform, strain-typical qualities independent of hearing.[46–48] Nevertheless, in the mouse, motor-related CD signals can be trained to suppress auditory cortical responses to arbitrary yet predictable acoustic consequences of locomotor or forelimb movements.[30,33,38] Therefore, an important goal of future studies will be to determine whether vocal modulation in the mouse auditory cortex displays flexibility that enables it to detect when the acoustic qualities of vocal feedback unexpectedly change. Such flexibility could provide the kernel of an adaptive mechanism that has been exploited for more complex vocal behaviors, including human speech.

Limitations of this study

The magnitude and timing of modulation by locomotor CD signals can be influenced by auditory feedback experience.[30,33,38] Therefore, the loss of vocalization- and locomotion-related auditory feedback experience may have contributed to differences we noted between neurons from hearing and deaf mice, such as smaller proportions of neurons modulated by vocalization or locomotion, enhanced magnitude of modulation, and a positive correlation between vocalization and locomotor modulation among neurons from deaf mice. More broadly, the auditory cortical circuit in deaf mice is likely altered by the absence of auditory experience across development.[49] To address these possibilities, future experiments could measure modulation by vocalization in mice after acutely inducing deafness.

In the present study and previous work, evidence to support the existence of vocal CD signals is gathered from the activity of auditory cortical neurons. The question of which neurons provide vocal CD signals to the auditory cortex remains to be addressed. By identifying these neurons and manipulating their activity during vocalization, future experiments could directly test whether vocal CD signals help the auditory cortex distinguish between the organism's own vocalizations and other sounds.

STAR★METHODS

RESOURCE AVAILABILITY

Lead contact—Further information and requests for resources and reagents should be directed to and will be fulfilled by the lead contact, Thomas Harmon (thomas.harmon@duke.edu).

Materials availability—This study did not generate any unique reagents.

Data and code availability

- No datasets comprised standardized datatypes in this study. Datasets of calcium imaging, audio recordings of vocalizations, and videos of orofacial movement and mouse interactions are available from the lead contact upon request.
- All original code, calcium fluorescence, behavioral measurements, and acoustic measurements are publicly available on Zenodo and may be accessed using the DOI listed in the key resources table.
- Any additional information required to reanalyze the data reported in this paper is available from the lead contact upon request.

EXPERIMENTAL MODEL AND STUDY PARTICIPANT DETAILS

Animals and husbandry—All surgical and experimental procedures were approved by the Duke University Institutional Animal Care and Use Committee. *Tmc1*$^{\Delta/\Delta}$ mice[39] (courtesy of Jeffery Holt, Harvard University) were crossed with *Vgat:Cre* mice (Jackson Labs #28862). Double heterozygous offspring were crossed with *Tmc1*$^{\Delta/\Delta}$ mice to generate mice that were either *Tmc1*$^{+/\Delta}$ (hearing) or *Tmc1*$^{\Delta/\Delta}$ (deaf) and *Cre*$^{+}$ or *Cre*$^{-}$. Mice were genotyped for *Cre* (Transnetyx) and the null *Tmc1* allele. Hearing was confirmed by measuring auditory brainstem responses to 1 ms click stimuli (>500 presentations), which were recorded with subdermal low-impendence monopolar electrodes (Technomed, TE/AP 2535), amplified with a microelectrode AC amplifier (AM Systems, Model 1800), and digitized with a Power 1401 data acquisition board at 10 kHz (Cambridge Electronic Design). Male *Cre*$^{+}$ mice (>60 days) were individually paired with a female mouse (>90 days, sexually experienced) for 10–20 days. During this time they received surgery and were habituated to head fixation. Mice were socially isolated for 3 days prior to imaging, and remained isolated for the duration of the experiment.

Imaging was conducted beginning 2–3 weeks after surgery and, for hearing mice, continued up to age 120 days to minimize the amount of data acquired after onset of degenerative hearing loss previously described in C57BL/6J mice.[51] This requirement was not applied to *Tmc1*$^{\Delta/\Delta}$ mice; consequently, the average age of *Tmc1*$^{\Delta/\Delta}$ mice used for imaging experiments was higher than *Tmc1*$^{+/\Delta}$ mice (178 ± 15 vs. 94 ± 9 days, $p < 0.001$). Other differences we noted were that, during head fixation, *Tmc1*$^{\Delta/\Delta}$ mice vocalized at slightly lower rates and had a vocal repertoire that deviated from repertoires of some hearing mice (Figure S5). These differences were not apparent in the USVs of unconstrained, age-matched *Tmc1*$^{+/\Delta}$ and *Tmc1*$^{\Delta/\Delta}$ mice (Figure 4B).

To maximize the likelihood that the mouse would vocalize while head-fixed, and to ensure that all USVs were produced by the head-fixed mouse, all experiments were conducted on sexually experienced male mice that were socially isolated prior to imaging. Male mice prepared in this way vocalize extensively during interactions with individual female mice. To assign USVs to the male, we considered the results of our airflow experiments. When negative airflow was applied and male odorants were drawn into the chamber containing the female mouse, no USVs were observed across 116 experiments. Conversely, USVs were numerous under positive airflow (i.e., Figures 2B and 2C), a condition in which

female odorants detectable by the male are likely increased. Female mice vocalize most readily to intruder females in their home cage or during interactions with multiple mice,[52,53] behavioral conditions which do not easily translate to head fixation. Nevertheless, we expect that the properties of vocal modulation (e.g., adaptive suppressive signature, prevocal onset) in the auditory cortex of male mice would be apparent in the auditory cortex of female mice as well, since these same properties have been previously reported in the auditory cortex of other species.[1,5–8,10,11,13,45]

All experiments were conducted during daylight hours. Female mice (60–120 days old) for inducing vocalization were co-housed with other females, and were sexually naive. The estrous cycle of these mice was not monitored, though we observed that across consecutive days (and presumably across estrous phases) the same female often elicited vocalizations from the same or different males. *Pv:Cre* (Jackson Labs #17320, $n = 3$) male mice were used for pilot experiments, and measurements of vocalization, orofacial movement, locomotion, and pupil size made from these mice during interaction with a female mouse were included (Figure 2; Figure S5).

METHOD DETAILS

Surgery—Mice were injected with dexamethasone (2 mg/mL, 2.8 mg/kg) 3 h prior to surgery to alleviate cerebral edema, cefazolin (125 mg/mL, 50 mg/kg) to prevent infection, meloxicam and topical bupivacaine for analgesia, and ketamine (50 mg/kg) and xylazine (5 mg/kg) for anesthesia, which was maintained with isoflurane (1%) after induction. Following exposure of the skull and implantation of a titanium 'Y' shaped headbar (H.E. Parmer) secured with metabond (Patterson Dental), the region overlying the left auditory cortex was marked stereotactically (AP: −2.8, ML: +4.4 from bregma) and softened by soaking with chilled buffer solution (142 mM NaCl, 5 mM KCl, 10 mM glucose, 10 mM HEPES, 3.1 mM $CaCl_2$, 1.3 mM $MgCl_2$, pH 7.2) for 5–10 min. A circular craniotomy (diameter = 2.6 mm) was made with a rotary drill (Dremel, bit size 5) by repeatedly applying the drill bit for 10–15 s then chilling with buffer solution. Viral vectors AAV2/9-*syn*-jGCaMP8s (Addgene #162374-AAV9) and AAV9.flex.tdTomato (Addgene #28306-AAV9) were combined in equal volumes, diluted 5x with buffer solution and biocompatible dye (Fast Green FCF, Sigma Aldrich), and loaded into a glass pipette. The tip of the pipette was inserted through the dura into the cortex (350–400 μm) where the virus was pressure injected (Nanoject III, Drummond Scientific; rate = 1 nL/s, volume = 40 nL/site). The spread of the dye-virus mixture was visually monitored. Following injection, the pipette was moved outside of the injected area and the procedure was repeated 8–10 times to completely distribute the virus across the craniotomy, which was subsequently covered with circular glass coverslips (Matsunami Glass; 3.0 mm disk glued to two 2.3 mm disks with Norland Optical Adhesive 71) secured into place with metabond and covered temporarily with silicon adhesive (Kwik-Sil, Prime Bioscience). Mice were returned to their home cage to recover. Meloxicam was injected again 12 h after surgery, while cefazolin was injected 3 times at 12-h increments.

Head-fixed courtship behavior—One week after receiving a headbar, mice were placed onto a radial treadmill with their head held stationary at a natural height and angle by

metal optical clamps (Thor Labs). A custom-built chamber (250 mL plastic bottle) with an approach corridor (50 mL Falcon tube with a 1 cm hole at the bottom) that extended to ~2 cm in front of the mouse's nose and a connecting airflow nozzle on the distal end was suspended above the treadmill. The mouse likely could not see the corridor and chamber, though it could likely detect the end of the corridor with its whiskers. Across several sessions (30–60 min in duration), mice habituated to head fixation. We observed that mice that did not spontaneously walk on the treadmill by the end of these sessions did not subsequently vocalize while head-fixed. Therefore, only animals that showed spontaneous bouts of walking were retained for subsequent imaging experiments. We also observed that male mice that vocalized reliably in darkness did not vocalize under low-luminance light. Consequently, habituation and imaging were conducted in the dark. Naive female mice were habituated to the chamber in the absence of the male for 2–3 sessions (~60 min, cumulatively).

Experimental sessions followed a pseudo-randomized block design in which calcium imaging was conducted from the male mouse while the female mouse was either absent, in a 'proximal' chamber immediately in front of the male, or in a second 'distal' chamber located ~50 cm from the male (1 L plastic bottle, with two connecting nozzles through the lid) that was connected to the proximal chamber. For positive and negative airflow conditions, pressurized air was directed through a flow meter (~2 L/min, Cole Parmer) to nozzles on the distal or proximal chambers. Across 16 mice and 116 experimental sessions, we observed vocalizations during social interaction in 59.5% of sessions, and no vocalizations when the mouse was socially isolated. Under these conditions, 84% of USV syllables were produced while the female was not in the approach corridor and interacting with the male, compared to 69% under neutral airflow conditions ($X^2(1, 135775) = 4298$, $p = 0.001$).

Two photon calcium imaging—We adapted a method for following locomotion speed during calcium imaging and sound presentation[33] to also follow pupil size, orofacial movement, female proximity, and vocalization. In this system, the mouse was head-fixed on top of a rotating disk that was mounted to a rotary encoder (US Digital), the output of which was streamed to a data acquisition card (National Instruments) connected to a computer (Dell) and sampled by custom MATLAB software (Mathworks, PsychToolBox) at 30 Hz. Sound stimuli were delivered using the same MATLAB program which controlled a sound card (RME Fireface 400, RME) that drove an ultrasonic speaker (Tucker Davis Technologies) located ~6 cm from the mouse's right ear. Calcium imaging was conducted using a resonant scanning two-photon microscope (Neurolabware) with a mode-locked titanium sapphire laser (Mai Tai DeepSee) at 920 nm (laser power levels: 80–100 mW). The microscope objective (16× 0.8 NA water immersion, Nikon) was rotated ~50° from vertical so that imaging was performed approximately orthogonal to the surface of the auditory cortex and imaging window while the mouse's head and body were at a neutral position. The space between the objective and the cranial window was filled with carbomer gel (refractive index = 1.4).

Emitted fluorescence from GCaMP8s (green) and tdTomato (red) was separated by a dichroic mirror and detected by separate photon magnifying tubes using software from Scanbox (sampling rate = 15.5 Hz) and saved as separate images (512 × 512 pixels).

Movement artifact in both channels was corrected using non-rigid registration (suite2p[54]) in which images of tdTomato fluorescence were divided into overlapping 128 × 128 pixel blocks, then the phase correlation between blocks from consecutive frames was maximized by shifting the subsequent image by < 12 pixels. Following co-registration of images from the two channels, putative neural regions of interest (ROIs) were detected automatically then manually inspected. ROIs were discarded if they were not somatic or if they showed evidence of residual movement contamination or saturated pixels. tdTomato$^+$ ROIs were identified through manual inspection. The somatic signal of each ROI was calculated as the mean fluorescence among all pixels comprising the ROI, while background neuropil fluorescence was calculated by suite2p from a set of bias functions that were localized to the same region of the field of view. Calcium time courses for each ROI were calculated as the somatic signal minus the product of the neuropil signal and a weighting coefficient (mean = 0.78, SD = 0.2), the value of which was determined algorithmically for each ROI to maximize the skewness of the resulting time course while ensuring no values below one.

Behavioral measurements during head fixation—Measurements of orofacial movements, shoulder movement, and pupil size were extracted from images (640 × 480 pixels) of the left side of the mouse's face and upper left forelimb. These images were gathered by a camera (Dalsa) that was triggered by the Scanbox software to be simultaneous with GCaMP8s sampling. Pupil size was measured using Facemap (https://github.com/MouseLand/FaceMap), which calculates the pixel area of an ellipse projected onto the pupil. Separate from our calcium imaging experiment, we measured the minimum and maximum pupil size from six mice in low and high background luminance conditions, then used these values to scale experimental values between 0 and 100%. Orofacial movements were measured as the proportion of the facial region of interest that showed a change in luminance, adjusted for noise of the camera. The region corresponding to the entire face, nose, whisker, jaw, or shoulder was manually identified in MATLAB and the number of pixels within each region that surpassed a threshold for change in luminance between consecutive frames (ΔP) was measured. The threshold was defined as the mean plus three standard deviations of ΔP for images gathered when the mouse was absent, meaning changes in luminance are solely attributable to sensor noise. Movement was then calculated from the equation $(\Delta P - P_{min})/(P_{max} - P_{min})$, where P_{min} was the modal ΔP for consecutive images during periods in which the mouse's speed was zero, and P_{max} was the total area of the region of interest. Movement time courses for each region of interest were constructed from movement measurements calculated for each frame.

The position of the female was recorded with a webcam (Logitech) directed toward the chamber and approach corridor. Using DeepLabCut (https://github.com/DeepLabCut), a classifier was trained on a subset of videos to identify the center of the female's torso and applied to the remainder of the dataset to generate pixel coordinates for each frame, then the distance between the coordinates and the end of the approach corridor was calculated. The resulting distance time course was downsampled and aligned to GCaMP8s images.

Audio recordings of vocalization—Audio recordings were made using an ultrasonic microphone located ~6 cm from the mouse's head (CM16/CMPA, Avisoft Bioacoustics).

Recordings were streamed to a computer via a pre-amplifier (Fireface 400, RME) and controller card (Firewire 1394), and sampled in MATLAB at 192 kHz. To identify USV syllables, recordings were high-pass filtered (40 kHz) and converted into sparse spectrograms (frequency resolution = 375 Hz). Following a previously developed procedure,[27] time points that met criteria for mean frequency (>40000), spectral purity (>0.3), and spectral discontinuity (<0.85) were identified. Consecutive time points within 30 ms of one another were considered to be a part of the same syllable, while consecutive syllables within 1 s of one another were considered to be a part of the same bout. After aligning syllable onset times to imaging frames, the instantaneous vocal rate was measured by calculating the inverse of the time interval between the onsets of consecutive syllables and interpolating the values into a time course that aligned with the GCaMP8s images.

To describe spectral qualities of individual syllables, a variational autoencoder (https://github.com/pearsonlab/autoencoded-vocal-analysis)[48] was trained on spectrograms of segmented USVs recorded during head-fixation or unconstrained courtship. The trained VAEs encoded a 32-dimensional latent embedding of each syllable, and a subset of embeddings were decoded and compared to original spectrograms to evaluate model performance. Uniform manifold approximation and projection[55] was applied to latent embeddings for further dimensionality reduction and visualization. Pairwise maximum mean discrepancy (MMD), implemented with an integral probability metric,[56] was used to quantify differences between syllable repertoires of individual mice. Band power, fundamental frequency, intensity, and entropy of sounds within the USV frequency band (36–96 kHz) were measured for the section of the recording that corresponded to each GCaMP8s image, and averaged across the first 2 s of vocalization or in 2 s-long sections of vocal epochs to describe vocal bouts. Vocal band power was measured as the decibel difference between each frame and the mean background power. The percentile of mean bandpower of vocal bouts was calculated relative to all other 2 s vocal epochs and categorized as ‘low’ (<33rd percentile), ‘mid’ (33rd to 67th), or ‘high’ (>67th). Primary frequency was defined as the frequency with the highest mean power, and intensity was defined as the decibel difference of the power of that frequency and the background. Entropy was defined as the quotient between the geometric mean and the arithmetic mean of the sound power in the USV frequency band.

Sound presentation—We presented tone pips (25 ms, 60 dB, 2–80 kHz, >20 presentations in pseudorandomized order) to male mice during spontaneous running and stillness in social isolation, presentation of odor from a distally-located female, and during social interaction and presentation of odor from a proximal female under positive airflow conditions. Best frequency was defined by the tone that drove a significant change in fluorescence that was more positive than all other tone responses presented while the mouse was socially isolated. During social isolation, we also presented USV playback stimuli, which were generated in one of two ways. The first set of stimuli, which were presented to all hearing mice (N = 6 stimuli, 2 s stimulus duration), were recorded during unrestrained social interaction between a female mouse and a male mouse with an ultrasonic microphone, streamed through a pre-amplifier (PreSonus V2 Tube), digitized at 192 kHz (Power 1401B, CED) recorded in Spike2 and denoised in Audacity. The second set of stimuli (N = 3–20

stimuli per day, 2 s duration, >10 presentation/stimulus) were generated from recordings collected during head-fixed social interaction and were presented later in the same imaging session. The raw recording was high-passed filtered at 40 kHz, rectified and smoothed with a median filter (10 ms wide), and putative vocal bout were identified as instances of sustained (>2 s) power that exceeded background noise. Stimuli were generated by excising the audio at each vocal bout onset, high-pass filtering (40 kHz), and denoising.

QUANTIFICATION AND STATISTICAL ANALYSIS

Identifying modulation with permutation tests—Permutation tests were conducted by first assigning a binary indicator code to each imaging frame for locomotion (running vs. not running), social interaction (female is present vs. is absent), female odor (female is in the proximal chamber under neutral or positive airflow or in the distal chamber with positive airflow vs. female absent or in the distal chamber under negative airflow), sound (during vs. separate from stimulus presentation), and vocalization (during vs. separate from a vocal bout). Next, epochs (i.e., consecutive frames) during which locomotion, sound, odor, or vocal modulation were ‘present’ or ‘absent’ were identified (i.e., Figures 1D and 3A). For all tests except for sound presentations, the duration of both ‘present’ and ‘absent’ epochs summed to at least 155 frames (10 s); otherwise, ROIs from those experiments were not included. Frames that did not meet the criterion for ‘absent’ or ‘present’ were not considered.

For locomotion, ‘present’ epochs were periods of running in social isolation, while ‘absent’ epochs were periods of stillness in social isolation. For sound, ‘present’ epochs were frames from 0 to 1 s following the presentation of a particular stimulus, while ‘absent’ epochs were frames when no sound was being presented, all in social isolation. While our data demonstrated otherwise, our *a priori* assumption was that the likelihood of locomotion would be influenced by social interaction and odor presentation, meaning that modulation by locomotion could obscure modulation by these other factors. Therefore, to measure modulation by vocalization and odor, we used frames during which the mouse’s locomotion state (i.e., running or still) was matched in the ‘present’ and ‘absent’ condition. For vocal modulation, ‘present’ epochs were periods when the male mouse was running and vocalizing and the female was in the proximal chamber in neutral or positive airflow conditions, while ‘absent’ epochs were periods of running with the female in the proximal chamber under neutral or positive airflow, but the male was not vocalizing. For odor modulation, ‘present’ epochs were periods of stillness during female odor presentation (i.e., positive airflow conditions with the female in the distal chamber), while ‘absent’ epochs were periods of stillness in social isolation. To address the possibility that odor and locomotion modulation interact, we also measured odor modulation by comparing periods of running during odor presentation and social isolation. We found that odor modulation measured during stillness correlated highly with odor modulation measured during running (Figure S3A).

For each ROI, the ‘dF’, (i.e., the difference between the mean fluorescence during ‘present’ and ‘absent’ sections) was calculated. To generate a null distribution to compare the dF value against, the labels for each epoch (‘present’ or ‘absent’) were shuffled 5000 times,

with the difference between the mean of epochs with each label calculated after shuffle. Modulated ROIs were defined as those with unshuffled values that were at least three standard deviations above or below the mean of the null distribution, corresponding to a false positive rate of 1%. This procedure is schematized in Figure 1D, along with an example of a positively modulated neuron. We found that the proportion of permutations that resulted in dF values above or below this threshold to be near 1% for all tests, well below the measured proportions of modulated neurons (Figures 3B and 4C).

Episodes of neural activation and suppression—dF/F was calculated from the neuropil-corrected fluorescence by the equation $dF/F = 100 * (F - F_0)/F0$, where $F0$ is the mean neuropil-corrected fluorescence from 2 to 1 s prior to behavioral onset or stimulus presentation. dF/F values were used to examine calcium activity at the onset of behavioral events or sound presentations, and to identify discrete episodes of activation and suppression during behavioral events. Thresholds of significantly increased or decreased dF/F values were calculated for each ROI from an imaging block when no stimuli were presented and the female mouse was absent by converting the fluorescence values to dF/F using a rolling window procedure. The values equal to two times the standard deviation of positive or negative dF/F values were used as the thresholds for activation and suppression. Putative suppressive episodes that occurred during the decay of positive calcium transients were excluded. Instances when the dF/F time course exceeded these thresholds were counted as episodes of activation or suppression and used for identifying activation and suppression near vocal onset and measurements of latency (i.e., Figures 1F–1H, 4E–4I, and 5H). Distributions of latency underwent kernel density smoothing with a bandwidth of 60 ms, the approximate duration of an imaging frame. For calculations of mean dF/F (i.e., Figures 1C, 1E, 3D and 3E, 4D and 4E, 4H and 4I, 5D and 5E, 5H, S1A, S1, S2A, S4), neurons were excluded in the number of events to which the dF/F calculation was aligned (e.g., vocal onset) did not exceed three.

Figures and statistical tests—Figure panels were generated in MATLAB 2023b and assembled in Adobe Illustrator. The graphical abstract was generated with BioRender. All statistical tests were conducted in MATLAB 2023b. All group summary statistics are reported as means and standard errors of the mean (SEM). Significant p-values are indicated in figures with asterisks: “*” is < 0.05, “**” is < 0.01, “***” is <0.001. Tests are reported in figure legends and detailed results are reported in Table S2. Repeated-measures analyses of variance (ANOVA) and posthoc Tukey-Kramer multiple comparisons of the estimated marginal means were used to compare trajectories of mean activity aligned to discrete events (i.e., vocal onset, locomotion onset, sound onset) across groups (i.e., pyramidal vs. interneuron, hearing vs. deaf). One-way ANOVAs were used to compare frequency, amplitude, and entropy across vocal bouts categorized by bandpower (i.e., Figure 5C). Two-way ANOVAs and Tukey-Kramer posthoc multiple comparisons tests were used to compare latency and magnitude across multiple conditions (i.e., neuron type and hearing status), and to compare mean fluorescence of neurons during vocal bouts with low, medium, or high bandpower and frequency (i.e., Figures 5D–5F). Measured proportions of co-modulated neurons were compared to a null hypothesis under which modulation factors are statistically independent from one another, and proportions of co-modulation are equal to the product

of proportions of neurons that exhibited modulation by each factor (reported in Figures 3B and 4C). Forms of co-modulation that fell outside of the 99% confidence interval of the null Chi-square distribution are indicated in Table S1.

Supplementary Material

Refer to Web version on PubMed Central for supplementary material.

ACKNOWLEDGMENTS

The authors would like to thank Professor Jeffery Holt (Harvard Medical School) for donating *Tmc1*$^{\Delta/\Delta}$ mice, Michael Booze for animal husbandry and genotyping, and Yang Lu for analytical assistance. They also thank Professor Steven Eliades, Dr. Shreyas M. Suryanarayana, and Katherine Kaplan for comments on the manuscript and all members of the Mooney lab for their helpful discussion and support. This research was supported by grants from the National Institutes of Health: F32 DC018721-01A1 (T.C.H.), R01DC013826-07 (R.M.), and R01MH117778-05 (R.M.).

REFERENCES

1. Müller-Preuss P, and Ploog D (1981). Inhibition of auditory cortical neurons during phonation. Brain Res. 215, 61–76. 10.1016/0006-8993(81)90491-1. [PubMed: 7260601]
2. Paus T, Perry DW, Zatorre RJ, Worsley KJ, and Evans AC (1996). Modulation of cerebral blood flow in the human auditory cortex during speech: role of motor-to-sensory discharges. Eur. J. Neurosci 8, 2236– 2246. 10.1111/j.1460-9568.1996.tb01187.x. [PubMed: 8950088]
3. Numminen J, and Curio G (1999). Differential effects of overt, covert and replayed speech on vowel-evoked responses of the human auditory cortex. Neurosci. Lett 272, 29–32. 10.1016/s0304-3940(99)00573-x. [PubMed: 10507535]
4. Curio G, Neuloh G, Numminen J, Jousmä ki V, and Hari R. (2000). Speaking modifies voice-evoked activity in the human auditory cortex. Hum. Brain Mapp. 9, 183–191. 10.1002/(sici)1097-0193(200004)9:4<183::aid-hbm1>3.0.co;2-z. [PubMed: 10770228]
5. Houde JF, Nagarajan SS, Sekihara K, and Merzenich MM (2002). Modulation of the auditory cortex during speech: an MEG study. J. Cognit. Neurosci 14, 1125–1138. 10.1162/089892902760807140. [PubMed: 12495520]
6. Eliades SJ, and Wang X (2003). Sensory-motor interaction in the primate auditory cortex during self-initiated vocalizations. J. Neurophysiol 89, 2194–2207. 10.1152/jn.00624.2002. [PubMed: 12612021]
7. Eliades SJ, and Wang X (2005). Dynamics of auditory-vocal interaction in monkey auditory cortex. Cerebr. Cortex 15, 1510–1523. 10.1093/cercor/bhi030.
8. Eliades SJ, and Wang X (2008). Neural substrates of vocalization feedback monitoring in primate auditory cortex. Nature 453, 1102–1106. 10.1038/nature06910. [PubMed: 18454135]
9. Ventura MI, Nagarajan SS, and Houde JF (2009). Speech target modulates speaking induced suppression in auditory cortex. BMC Neurosci. 10, 58. 10.1186/1471-2202-10-58. [PubMed: 19523234]
10. Flinker A, Chang EF, Kirsch HE, Barbaro NM, Crone NE, and Knight RT (2010). Single-trial speech suppression of auditory cortex activity in humans. J. Neurosci 30, 16643–16650. 10.1523/JNEUROSCI.1809-10.2010. [PubMed: 21148003]
11. Behroozmand R, and Larson CR (2011). Error-dependent modulation of speech-induced auditory suppression for pitch-shifted voice feedback. BMC Neurosci. 12, 54. 10.1186/1471-2202-12-54. [PubMed: 21645406]
12. Eliades SJ, and Wang X (2017). Contributions of sensory tuning to auditory-vocal interactions in marmoset auditory cortex. Hear. Res 348, 98–111. 10.1016/j.heares.2017.03.001. [PubMed: 28284736]

13. Knolle F, Schwartze M, Schröger E, and Kotz SA. (2019). Auditory Predictions and Prediction Errors in Response to Self-Initiated Vowels. Front. Neurosci 13, 1146. 10.3389/fnins.2019.01146. [PubMed: 31708737]

14. Schneider DM, Nelson A, and Mooney R (2014). A synaptic and circuit basis for corollary discharge in the auditory cortex. Nature 513, 189–194. 10.1038/nature13724. [PubMed: 25162524]

15. Lin P-A, Asinof SK, Edwards NJ, and Isaacson JS (2019). Arousal regulates frequency tuning in primary auditory cortex. Proc. Natl. Acad. Sci. USA 116, 25304–25310. 10.1073/pnas.1911383116. [PubMed: 31757852]

16. McGinley MJ, David SV, and McCormick DA (2015). Cortical Membrane Potential Signature of Optimal States for Sensory Signal Detection. Neuron 87, 179–192. 10.1016/j.neuron.2015.05.038. [PubMed: 26074005]

17. Nelson A, and Mooney R (2016). The Basal Forebrain and Motor Cortex Provide Convergent yet Distinct Movement-Related Inputs to the Auditory Cortex. Neuron 90, 635–648. 10.1016/j.neuron.2016.03.031. [PubMed: 27112494]

18. Nelson A, Schneider DM, Takatoh J, Sakurai K, Wang F, and Mooney R (2013). A circuit for motor cortical modulation of auditory cortical activity. J. Neurosci 33, 14342–14353. 10.1523/JNEUROSCI.2275-13.2013. [PubMed: 24005287]

19. McGinley MJ, Vinck M, Reimer J, Batista-Brito R, Zagha E, Cadwell CR, Tolias AS, Cardin JA, and McCormick DA (2015). Waking State: Rapid Variations Modulate Neural and Behavioral Responses. Neuron 87, 1143–1161. 10.1016/j.neuron.2015.09.012. [PubMed: 26402600]

20. Clayton KK, Williamson RS, Hancock KE, Tasaka GI, Mizrahi A, Hackett TA, and Polley DB (2021). Auditory Corticothalamic Neurons Are Recruited by Motor Preparatory Inputs. Curr. Biol 31, 310–321.e5. 10.1016/j.cub.2020.09.021. [PubMed: 33157020]

21. Cohen L, Rothschild G, and Mizrahi A (2011). Multisensory integration of natural odors and sounds in the auditory cortex. Neuron 72, 357–369. 10.1016/j.neuron.2011.08.019. [PubMed: 22017993]

22. Gilday OD, and Mizrahi A (2023). Learning-Induced Odor Modulation of Neuronal Activity in Auditory Cortex. J. Neurosci 43, 1375–1386. 10.1523/JNEUROSCI.1398-22.2022. [PubMed: 36650061]

23. Cohen L, and Mizrahi A (2015). Plasticity during motherhood: changes in excitatory and inhibitory layer 2/3 neurons in auditory cortex. J. Neurosci 35, 1806–1815. 10.1523/JNEUROSCI.1786-14.2015. [PubMed: 25632153]

24. Sales (née Sewell) GDS. (1972). Ultrasound and mating behaviour in rodents with some observations on other behavioural situations. J. Zool 168, 149–164. 10.1111/j.1469-7998.1972.tb01345.x.

25. Whitney G, Alpern M, Dizinno G, and Horowitz G (1974). Female odors evoke ultrasounds from male mice. Anim. Learn. Behav 2, 13–18. 10.3758/bf03199109. [PubMed: 4468889]

26. Sipos ML, Kerchner M, and Nyby JG (1992). An ephemeral sex pheromone in the urine of female house mice (Mus domesticus). Behav. Neural. Biol 58, 138–143. 10.1016/0163-1047(92)90375-e. [PubMed: 1456933]

27. Holy TE, and Guo Z (2005). Ultrasonic songs of male mice. PLoS Biol. 3, e386. 10.1371/journal.pbio.0030386. [PubMed: 16248680]

28. Seagraves KM, Arthur BJ, and Egnor SER (2016). Evidence for an audience effect in mice: male social partners alter the male vocal response to female cues. J. Exp. Biol 219, 1437–1448. 10.1242/jeb.129361. [PubMed: 27207951]

29. Tschida K, Michael V, Takatoh J, Han BX, Zhao S, Sakurai K, Mooney R, and Wang F (2019). A Specialized Neural Circuit Gates Social Vocalizations in the Mouse. Neuron 103, 459–472.e4. 10.1016/j.neuron.2019.05.047. [PubMed: 31204083]

30. Audette NJ, Zhou W, La Chioma A, and Schneider DM (2022). Precise movement-based predictions in the mouse auditory cortex. Curr. Biol 32, 4925–4940.e6. 10.1016/j.cub.2022.09.064. [PubMed: 36283411]

31. Zhou M, Liang F, Xiong XR, Li L, Li H, Xiao Z, Tao HW, and Zhang LI (2014). Scaling down of balanced excitation and inhibition by active behavioral states in auditory cortex. Nat. Neurosci 17, 841–850. 10.1038/nn.3701. [PubMed: 24747575]
32. Rummell BP, Klee JL, and Sigurdsson T (2016). Attenuation of Responses to Self-Generated Sounds in Auditory Cortical Neurons. J. Neurosci 36, 12010–12026. 10.1523/JNEUROSCI.1564-16.2016. [PubMed: 27881785]
33. Schneider DM, Sundararajan J, and Mooney R (2018). A cortical filter that learns to suppress the acoustic consequences of movement. Nature 561, 391–395. 10.1038/s41586-018-0520-5. [PubMed: 30209396]
34. Bigelow J, Morrill RJ, Dekloe J, and Hasenstaub AR (2019). Movement and VIP Interneuron Activation Differentially Modulate Encoding in Mouse Auditory Cortex. eNeuro 6, 1–14. 10.1523/ENEURO.0164-19.2019.
35. Henschke JU, Price AT, and Pakan JMP (2021). Enhanced modulation of cell-type specific neuronal responses in mouse dorsal auditory field during locomotion. Cell Calcium 96, 102390. 10.1016/j.ceca.2021.102390.
36. Vivaldo CA, Lee J, Shorkey M, Keerthy A, and Rothschild G (2023). Auditory cortex ensembles jointly encode sound and locomotion speed to support sound perception during movement. PLoS Biol. 21, e3002277. 10.1371/journal.pbio.3002277.
37. Morandell K, Yin A, Triana Del Rio R, and Schneider DM (2024). Movement-related modulation in mouse auditory cortex is widespread yet locally diverse. J. Neurosci 44, e1227232024. 10.1523/JNEUROSCI.1227-23.2024.
38. Audette NJ, and Schneider DM (2023). Stimulus-Specific Prediction Error Neurons in Mouse Auditory Cortex. J. Neurosci 43, 7119–7129. 10.1523/JNEUROSCI.0512-23.2023. [PubMed: 37699716]
39. Kawashima Y, Géléoc GSG, Kurima K, Labay V, Lelli A, Asai Y, Makishima T, Wu DK, Della Santina CC, Holt JR, and Griffith AJ. (2011). Mechanotransduction in mouse inner ear hair cells requires transmembrane channel-like genes. J. Clin. Invest 121, 4796–4809. 10.1172/JCI60405. [PubMed: 22105175]
40. Zheng DJ, Okobi DE Jr., Shu R, Agrawal R, Smith SK, Long MA, and Phelps SM (2022). Mapping the vocal circuitry of Alston's singing mouse with pseudorabies virus. J. Comp. Neurol 530, 2075–2099. 10.1002/cne.25169. [PubMed: 35385140]
41. Riede T (2014). Rat ultrasonic vocalization shows features of a modular behavior. J. Neurosci 34, 6874–6878. 10.1523/JNEURO-SCI.0262-14.2014. [PubMed: 24828641]
42. Riede T (2018). Peripheral Vocal Motor Dynamics and Combinatory Call Complexity of Ultrasonic Vocal Production in Rats. In Handbook of Behavioral Neuroscience, 25 (Elsevier), pp. 45–60. 10.1016/B978-0-12-809600-0.00005-6.
43. Okobi DE Jr., Banerjee A, Matheson AMM, Phelps SM, and Long MA (2019). Motor cortical control of vocal interaction in neotropical singing mice. Science 363, 983–988. 10.1126/science.aau9480. [PubMed: 30819963]
44. Hickok G, Houde J, and Rong F (2011). Sensorimotor integration in speech processing: computational basis and neural organization. Neuron 69, 407–422. 10.1016/j.neuron.2011.01.019. [PubMed: 21315253]
45. Houde JF, and Jordan MI (1998). Sensorimotor adaptation in speech production. Science 279, 1213–1216. 10.1126/science.279.5354.1213. [PubMed: 9469813]
46. Hammerschmidt K, Reisinger E, Westekemper K, Ehrenreich L, Strenzke N, and Fischer J (2012). Mice do not require auditory input for the normal development of their ultrasonic vocalizations. BMC Neurosci. 13, 40. 10.1186/1471-2202-13-40. [PubMed: 22533376]
47. Mahrt EJ, Perkel DJ, Tong L, Rubel EW, and Portfors CV (2013). Engineered deafness reveals that mouse courtship vocalizations do not require auditory experience. J. Neurosci 33, 5573–5583. 10.1523/JNEUROSCI.5054-12.2013. [PubMed: 23536072]
48. Goffinet J, Brudner S, Mooney R, and Pearson J (2021). Low-dimensional learned feature spaces quantify individual and group differences in vocal repertoires. Elife 10, e67855. 10.7554/eLife.67855.

49. Kral A, Popper AN, and Fay RR, eds. (2013). Deafness. Springer, pp. 47–198. 10.1007/978-1-4614-7840-9.
50. Zhang Y, Rózsa M, Bushey D, Zheng J, Reep D, Broussard GJ, Tsang A, Tsegaye G, Patel R, Narayan S, et al. (2020). jGCaMP8 Fast Genetically Encoded Calcium Indicators. Janelia Research Campus 10, 13148243. 10.25378/janelia.13148243.
51. Henry KR, and Chole RA (1980). Genotypic differences in behavioral, physiological and anatomical expressions of age-related hearing loss in the laboratory mouse. Audiology 19, 369–383. 10.3109/00206098009070071. [PubMed: 7436856]
52. Neunuebel JP, Taylor AL, Arthur BJ, and Egnor SER (2015). Female mice ultrasonically interact with males during courtship displays. Elife 4, e06203. 10.7554/eLife.06203.
53. Zhao X, Ziobro P, Pranic NM, Chu S, Rabinovich S, Chan W, Zhao J, Kornbrek C, He Z, and Tschida KA (2021). Sex- and context-dependent effects of acute isolation on vocal and non-vocal social behaviors in mice. PLoS One 16, e0255640. 10.1371/journal.pone.0255640.
54. Pachitariu M, Stringer C, Schröder S, Schröder S, Rossi LF, Dalgleish H, Carandini M, and Harris KD (2016). Suite2p: beyond 10,000 neurons with standard two-photon microscopy. Preprint at bioRxiv, 061507. 10.1101/061507.
55. McInnes L, Healy J, and Melville J (2018). UMAP: Uniform Manifold Approximation and Projection for Dimension Reduction. Preprint at arXiv, 1–63. 10.48550/arXiv.1802.03426.
56. Gretton A, Borgwardt KM, Rasch MJ, Schölkopf B, and Smola A. (2012). A kernel two-sample test. J. Mach. Learn. Res 13, 723–773.

Highlights

- Vocal production suppresses the auditory cortex of both hearing and deaf mice
- Vocal modulation is distinct from modulatory effects of locomotion and olfaction
- Vocal modulation scales with vocal power and complexity in hearing and deaf mice
- Vocal modulation bears the hallmarks of an adaptive corollary discharge mechanism

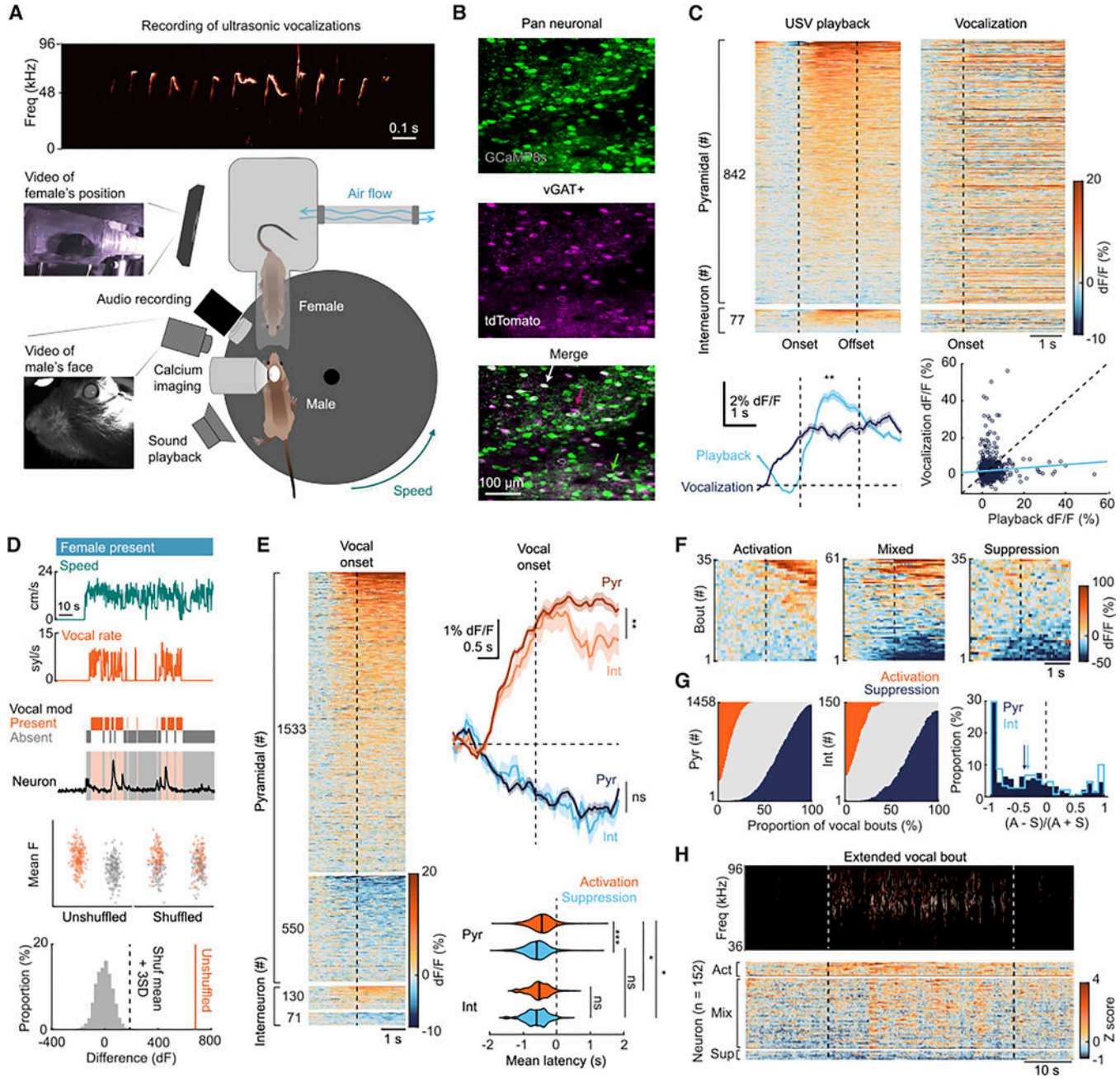

Figure 1. Vocalization modulates the mouse auditory cortex

(A) Schematic of experimental protocol.

(B) Max projection of the GCaMP8s signal (top), tdTomato signal (middle), and both signals merged (bottom) from an example field of view. Green arrow, putative pyramidal neuron. White, interneuron with GCaMP8s. Magenta, interneuron without GCaMP8s.

(C) Top, mean dF/F of neurons that responded to ≥ 1 USV playback stimulus aligned to presentations of all playback stimuli (left) and vocalization (right) ordered by magnitude of playback dF/F. Bottom left, mean dF/F ± SEM aligned to playback (light) and vocalization (dark). Asterisks, significant difference (repeated-measures ANOVA): *$p < 0.05$; **$p < 0.01$;

and ***$p < 0.001$. Bottom right, mean dF/F during playback plotted against mean dF/F during vocalization. Blue line, linear fit. Dashed line, unity. See also Figure S1.

(D) Schematic of permutation procedure. Top, time courses of female presence (binary), speed, and vocal rate. Middle, epochs when vocal modulation was present (orange) or absent (gray) and fluorescence from a modulated neuron. Bottom, markers, mean fluorescence for each epoch during which vocal modulation was present or absent, before and after shuffling, and the distribution of differences between the means of shuffled fluorescence values and the unshuffled difference value. Dotted line, threshold for considering the neuron positively modulated.

(E) Left, mean dF/F of vocalization-modulated pyramidal (top) and interneurons (bottom) at vocal onset sorted into groups with positive or negative values and ordered by absolute magnitude. Right, mean ± SEM dF/F of pyramidal (dark shade) or interneurons (light) that show positive (orange) or negative (blue) values. Stats, repeated-measures ANOVA. Bottom, kernel-smoothed distributions of mean latencies of activation or suppression relative to vocalization onset for individual pyramidal neurons (top) or interneurons (bottom). Black line, group mean. Stats, ANOVA with Tukey-Kramer test.

(F) dF/F aligned to onset of single vocal bouts and ordered by mean amplitude of three example neurons that show bouts with activation (left), suppression (right), or either activation or suppression (mixture, center).

(G) Proportions of vocal bouts (−2 to +2 s from onset) during which significant activation (orange), suppression (blue), or no significant dF/F (gray) was detected in pyramidal (left) or interneurons (right). Right, distribution of difference between the number of activation and suppression episodes divided by the sum of episodes. −1, neuron only shows suppression during vocalization. +1, neuron only shows activation. Arrows, group means.

(H) Top, spectrogram of a long-duration (~40 s) vocal bout. Bottom, fluorescence of vocalization-modulated neurons ordered by mean fluorescence during vocalization.

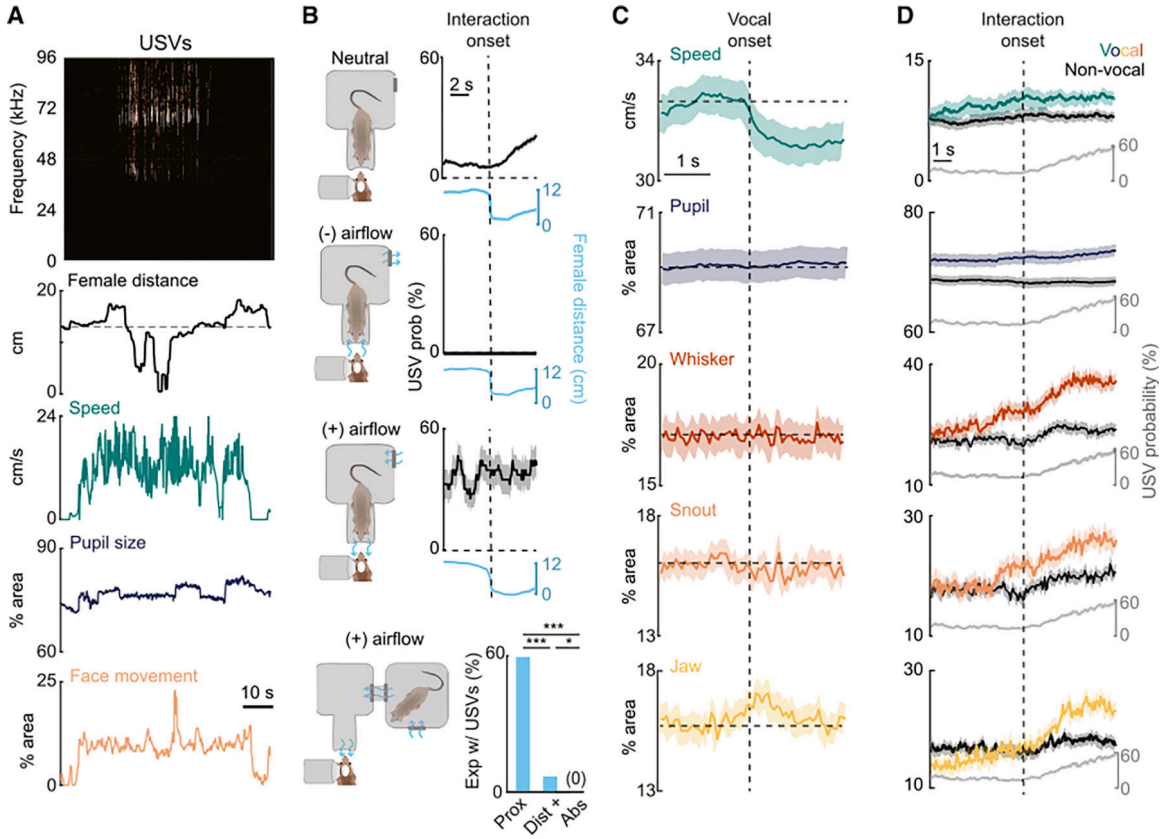

Figure 2. Behavioral correlates of vocalization

(A) Top to bottom, USVs, female distance (dashed line, threshold of interaction), speed, pupil size, and face movement of the male mouse during a social interaction.

(B) Left, schematics showing position of male and female mice and direction of airflow in each condition. Right, vocalization probability (black line) and female position (blue) aligned to female approach under neutral (top), negative (middle), or positive (bottom) airflow. Bottom right, proportion of experiments in which USVs were present while the female was in the proximal chamber under neural airflow (Prox), in the distal chamber with positive airflow (Dist, +), or absent (Abs). Stats, chi-squared test with Bonferroni correction. Asterisks, *$p < 0.05$; **$p < 0.01$; and ***$p < 0.001$. For all images, $N = 13$ mice, 116 sessions.

(C) Mean ± SEM of speed, pupil size, and movement of the whisker pad, snout, or jaw aligned to vocalization onset (vertical dashed line). Horizontal line, baseline.

(D) Mean ± SEM of measurements in (C) and USV probability aligned to when the female enters the approach corridor (Interaction onset, vertical line) that did (colored) or did not (black) coincide with USVs.

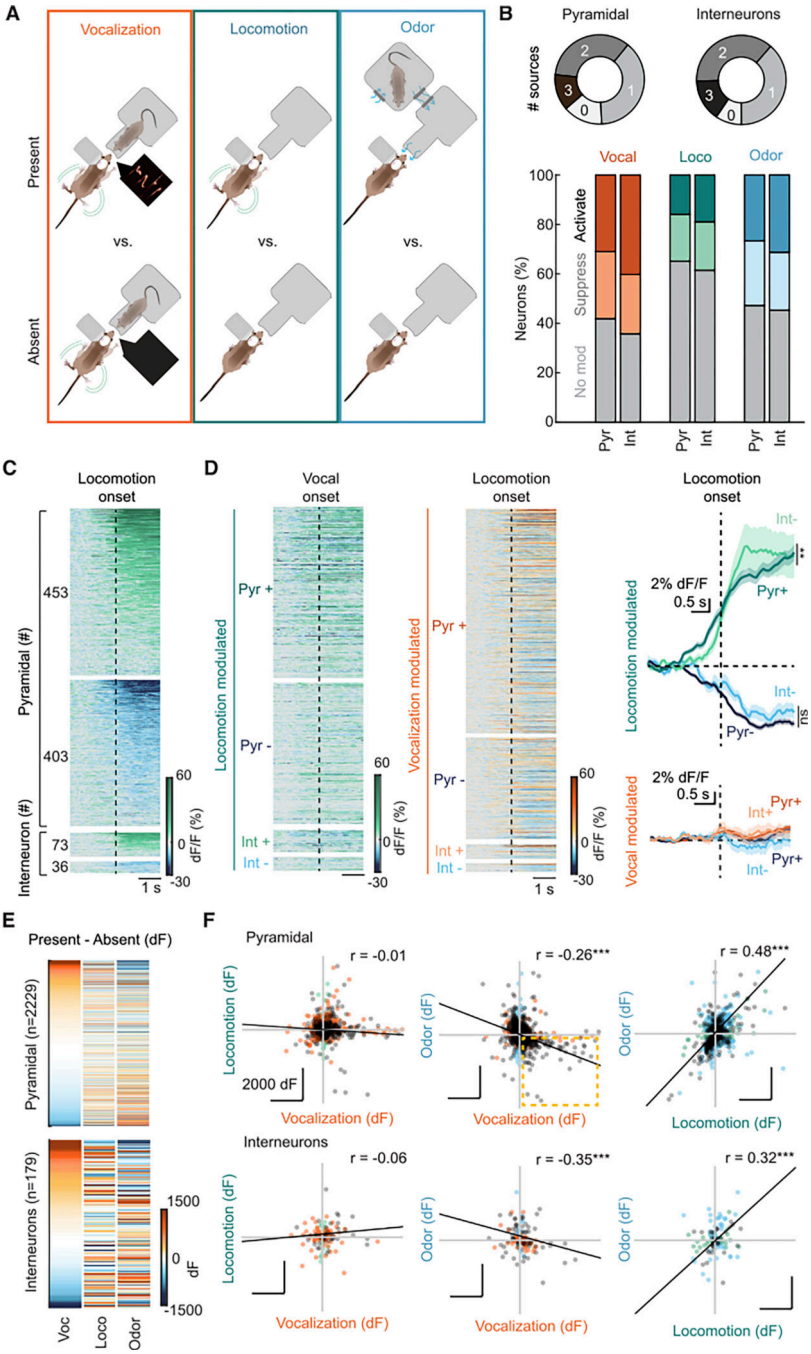

Figure 3. Dissociating vocal modulation from locomotor and odor modulation

(A) Schematics of conditions used to detect modulation in which vocalization (left), locomotion (center), or odor (right) modulation was coded as present or absent.

(B) Top, proportion of pyramidal or interneurons that were significantly modulated by 0–3 sources. Bottom, proportions of pyramidal or interneurons that were activated, suppressed, or unmodulated by vocalization, locomotion, or female odor. $N = 2{,}229$ pyramidal neurons, 179 interneurons.

(C) Mean dF/F of locomotion-modulated pyramidal (top) and interneurons (bottom) at locomotion onset sorted into groups with positive or negative values and ordered by absolute magnitude.

(D) Left, mean dF/F of neurons that were activated (+) or suppressed (−) by locomotion at vocal onset. Same neurons and ordering as (D). Center, mean dF/F of vocalization-modulated neurons at locomotion onset. Same neurons and ordering as Figure 1E. Right, mean ± SEM dF/F of locomotion-modulated (top) or vocalization-modulated (bottom) pyramidal (dark shade) or interneurons (light) that show positive (green/orange) or negative values. Stats, repeated-measures ANOVA. *$p < 0.05$; **$p < 0.01$; and ***$p < 0.001$.

(E) Vocalization, locomotion, and odor dF among pyramidal neurons (left) and interneurons (right) ordered by magnitude of vocal dF.

(F) Pairwise comparisons and Pearson correlations of differences between mean fluorescence during present and absent epochs (dF) for vocalization, locomotion, and odor. Colored markers, neurons significantly modulated by only vocalization (orange), locomotion (green), or odor (blue). Black markers, modulated by both factors. Black line, linear fit of black markers. Yellow box, neurons activated by vocalization and suppressed by odor. Unmodulated neurons are not plotted but are included in the correlation calculation.

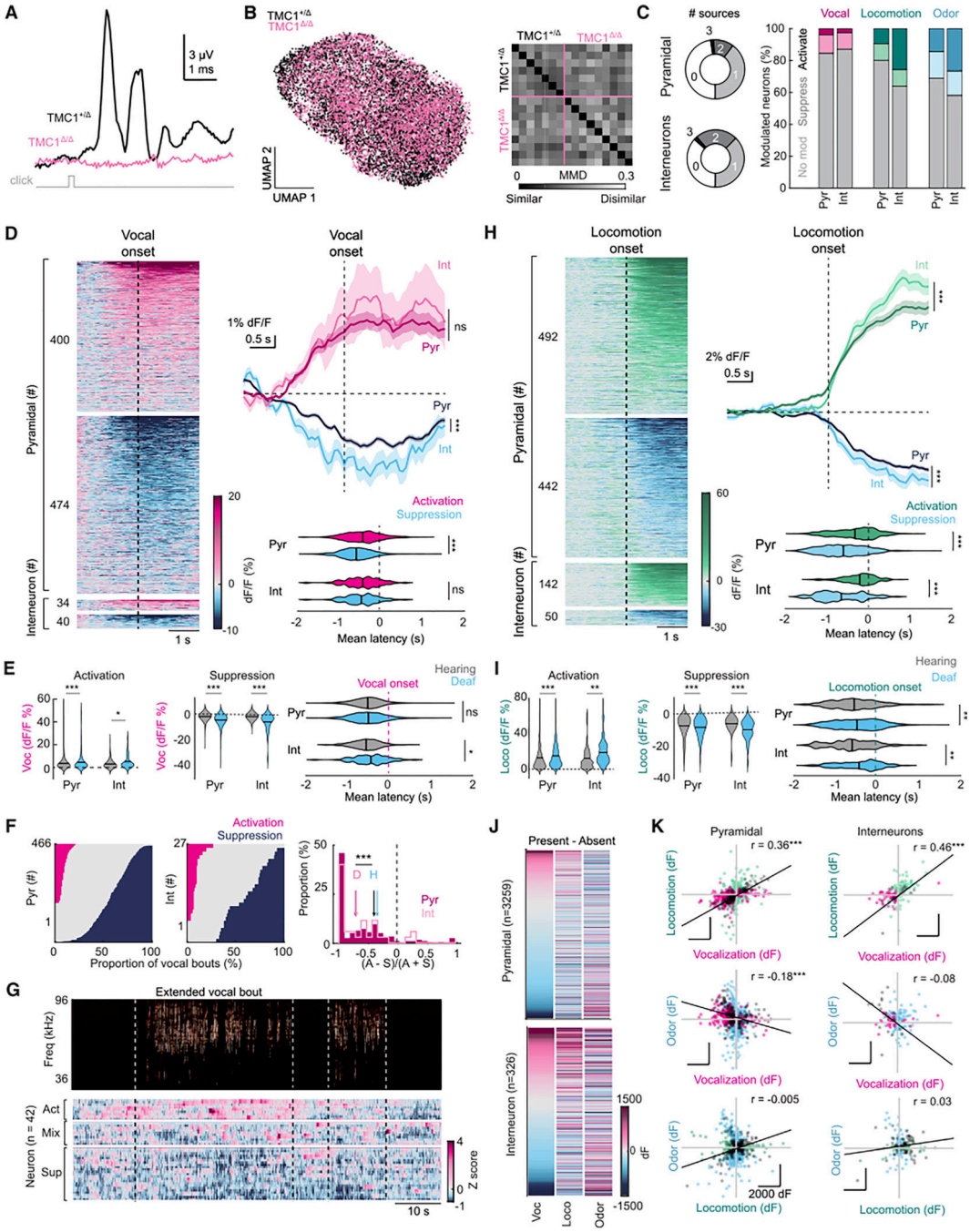

Figure 4. Vocal and non-vocal modulation of auditory cortical neurons in deaf mice

(A) Mean auditory brainstem responses to a brief click stimulus (1 ms) collected from a hearing (*Tmc1*$^{+/\Delta}$, black) and a deaf (*Tmc1*$^{\Delta/\Delta}$, pink) mouse.

(B) Left, projections of the uniform manifold approximation of latent values that represent the spectral features of USV syllables (N = 12,780) generated by hearing (black) or deaf (pink) mice. Right, similarity matrix between pairs of syllable repertoires of individual hearing or deaf mice, as captured by the maximum mean discrepancy.

(C) Same as Figure 3B but for neurons from deaf mice. See also Figure S5B.

(D) Same as Figure 1E but for neurons from deaf mice. Stats, repeated-measures ANOVA (mean dF/F) and ANOVA with Tukey-Kramer test (latency). *$p < 0.05$; **$p < 0.01$; and ***$p < 0.001$.

(E) Distribution of the mean dF/F magnitude and mean latencies of episodes of activation or suppression of auditory cortical neurons relative to vocal onset among auditory cortical neurons from hearing (gray) or deaf (blue) mice that were activated or suppressed by vocalization. Black line, group mean. Stats, ANOVA with Tukey-Kramer test. *N*, hearing = 2,083 pyramidal neurons, 201 interneurons, 4,858 episodes; deaf = 874 pyramidal, 74 interneurons, and 2,376 episodes.

(F and G) Same as Figures 1G and 1H but for neurons from deaf mice. Magenta arrows, means of deaf group. Blue arrows, means of pyramidal (dark) and interneurons (light) from hearing mice. Stats, ANOVA with Tukey-Kramer test.

(H) Mean dF/F of locomotion-modulated pyramidal (top) and interneurons (bottom) from deaf mice at locomotion onset sorted into those with positive or negative values and ordered by absolute magnitude. Right top, mean ± SEM dF/F of pyramidal (dark shade) or interneurons (light) with positive (green) or negative (blue) values. Right bottom, distribution of mean latencies after kernel density smoothing of activation or suppression relative to locomotion onset for individual pyramidal neurons (top) or interneurons (bottom). Black line, group mean. Stats, repeated-measures ANOVA (mean dF/F) and ANOVA with Tukey-Kramer test (latency). See also Figure S4.

(I) Same as (E) but among locomotion-modulated neurons, relative to locomotion onset. Stats, ANOVA with Tukey-Kramer test. *N*, hearing = 856 pyramidal neurons, 109 interneurons, 1,818 episodes; deaf = 934 pyramidal, 192 interneurons, and 2,129 episodes.

(J and K) Same as Figures 3F and 3G but for neurons from deaf mice. Stats, pairwise Pearson correlations.

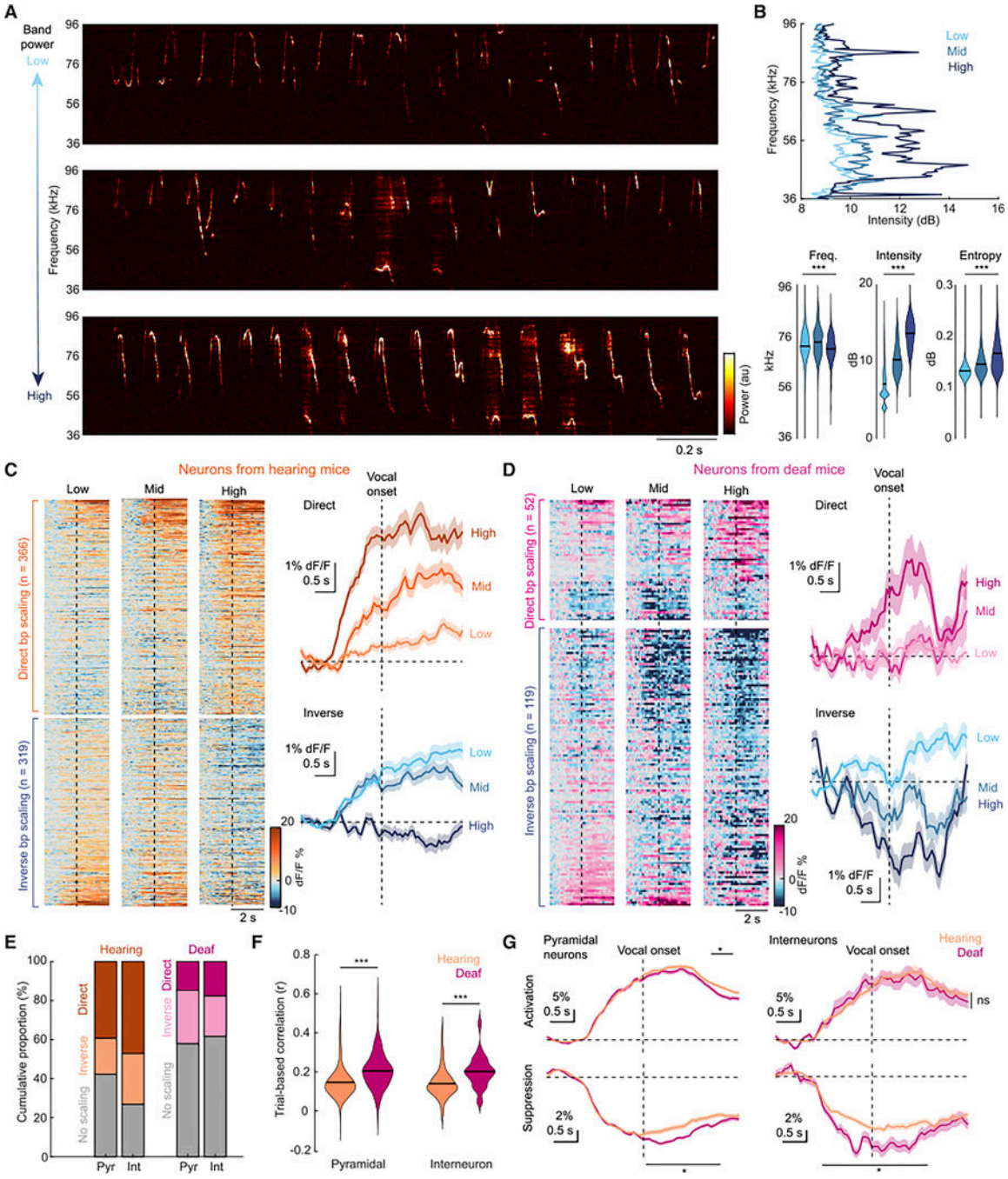

Figure 5. Vocal modulation scales with band power in the auditory cortex of hearing and deaf mice

(A) Spectrograms of the first 2 s of vocal bouts from the same mouse with mean band power values in the low third ("low," top), middle third ("mid," center), or high third ("high," top) of all recordings in the dataset.

(B) Top, relationship between sound frequency and intensity for the spectrograms in (A). Bottom, distributions of mean frequency (left), sound intensity (middle), and entropy (right) of 1 s vocal block with low, mid, or high band powers. Stats, one-way ANOVA. *$p < 0.05$; **$p < 0.01$; and ***$p < 0.001$. $N = 152{,}961$ blocks.

(C) Left, mean dF/F of individual vocalization-modulated neurons that showed significant scaling to band power aligned to low, mid, or high band power vocal bouts sorted by whether the dF/F increases (direct) or decreases (inverse) with increasing band power and ordered by magnitude during high-band-power bouts. Vertical dashed line, vocal onset. Right, mean ± SEM dF/F aligned to onset of low-, mid-, or high-band-power bouts among neurons that show direct (orange, top) or inverse (blue, bottom) band power scaling.
(D) Same as (C) but for neurons from deaf mice.
(E) Proportions of pyramidal and interneurons that show significant direct or inverse scaling, or no significant scaling, in hearing (orange, throughout) and deaf (magenta, throughout) mice.
(F) Distribution of mean trial-based correlations, calculated between the single vocal bout dF/F and the mean dF/F, among pyramidal (left) and interneurons (right) from hearing and deaf mice. Stats, ANOVA with Tukey-Kramer test.
(G) Group mean ± SEM dF/F for vocal bouts with episodes of significant activation (top) or suppression (bottom) among pyramidal neurons (left) or interneurons (right) from hearing and deaf mice. Stats, repeated-measures ANOVA with Tukey-Kramer test.

Cell Rep. Author manuscript; available in PMC 2025 January 10.

KEY RESOURCES TABLE

REAGENT or RESOURCE	SOURCE	IDENTIFIER
Bacterial and virus strains		
AAV2/9-*syn*-jGCaMP8s-WPRE	GENIE Project; Zhang et al.[50]	Addgene 162374-AAV9
AAV9.FLEX.tdTomato	Edward Boyden	Addgene 28306-AAV9
Critical commercial assays		
DNeasy Blood and Tissue Kit	Qiagen	Cat. # 69504
Deposited data		
Calcium fluorescence, behavioral measurements, and acoustic measurements	This study	https://doi.org/10.5281/zenodo.10946465
Experimental models: Organisms/strains		
C57BL/6J, B6J.129S6(FVB)-Slc32a1tm2 (cre)Lowl/MwarJ, Vgat:Cre	Jackson Labs	RRID:IMSR_JAX:028862
C57BL/6J, B6.129P2-Pvalbtm1 (cre)Arbr/J, Pv:Cre	Jackson Labs	RRID:IMSR_JAX:017320
C57BL/6J, $Tmc1^{\Delta/\Delta}$, $Tmc1^{\Delta/\Delta}$	Donated by Jeffery Holt (Harvard Medical School); ref. 39	N/A
Software and algorithms		
MATLAB	Mathworks	RRID:SCR_001622
Spike2	Cambridge Electronic Design	RRID:SCR_000903
Scanbox	Neurolabware; https://scanbox.org/	N/A
suite2p	https://github.com/MouseLand/suite2p	RRID:SCR_016434
Deeplabcut	https://github.com/DeepLabCut/DeepLabCut	RRID:SCR_021391
Facemap	https://github.com/MouseLand/facemap	RRID:SCR_021513
AVA	https://github.com/pearsonlab/autoencoded-vocal-analysis	N/A